

This article is licensed under a Creative Commons Attribution-NonCommercial NoDerivatives 4.0 International License.

## Betulinic Acid Inhibits Cell Proliferation in Human Oral Squamous Cell Carcinoma via Modulating ROS-Regulated p53 Signaling

Huan Shen,<sup>\*1</sup> Li Liu,<sup>†1</sup> Yongjin Yang,<sup>\*</sup> Wenxing Xun,<sup>‡</sup> Kewen Wei,<sup>‡</sup> and Guang Zeng<sup>‡</sup>

<sup>\*</sup>Department of Stomatology, The General Hospital of the Second Artillery Corps of Chinese PLA, Beijing, P.R. China

<sup>†</sup>Department of Stomatology, PLA Army General Hospital, Beijing, P.R. China

<sup>‡</sup>Department of Plastic and Burn Surgery, Tangdu Hospital, Fourth Military Medical University, Xi'an, P.R. China

Oral squamous cell carcinoma (OSCC) is a common cancer of the head and neck. Betulinic acid (BA) is a naturally occurring pentacyclic triterpenoid. The present study was designed to explore the effects of BA on OSCC KB cell proliferation in vitro and on implanted tumor growth in vivo and to examine the possible molecular mechanisms. The results showed that BA dose-dependently inhibited KB cell proliferation and decreased implanted tumor volume. In addition, BA significantly promoted mitochondrial apoptosis, as reflected by an increase in TUNEL<sup>+</sup> cells and the activities of caspases 3 and 9, an increase in Bax expression, and a decrease in Bcl-2 expression and the mitochondrial oxygen consumption rate. BA significantly increased cell population in the G<sub>0</sub>/G<sub>1</sub> phase and decreases the S phase cell number, indicating the occurrence of G<sub>0</sub>/G<sub>1</sub> cell cycle arrest. ROS generation was significantly increased by BA, and antioxidant NAC treatment markedly inhibited the effect of BA on apoptosis, cell cycle arrest, and proliferation. BA dose-dependently increased p53 expression in KB cells and implanted tumors. p53 reporter gene activity and p53 binding in the promoters of Bax were significantly increased by BA. Knockdown of p53 blocked BA-induced increase in apoptosis, cell cycle arrest, and inhibition of cell proliferation. NAC treatment suppressed BA-induced increase in p53 expression. Furthermore, phosphorylation of signal transducer and activator of transcription 3 (STAT3) was increased by BA. Taken together, the data demonstrated that ROS-p53 signaling was crucial for BA-exhibited antitumor effect in OSCC. BA may serve as a potential drug for the treatment of oral cancer.

**Key words: Betulinic acid (BA); Oral squamous cell carcinoma (OSCC); Apoptosis; Cell cycle arrest; p53; Signal transducer and activator of transcription 3 (STAT3); Reactive oxygen species (ROS)**

### INTRODUCTION

Oral squamous cell carcinoma (OSCC) is believed to be one of the most common cancers of the head and neck region<sup>1</sup>, accounting for approximately 90% of diagnosed patients with oral cancer<sup>2</sup>. In the past few years, there have been great advances in surgery and radiotherapy for OSCC. However, OSCC is commonly recurrent, leading to a poor prognosis, with less than 50% having a 5-year survival rate<sup>1</sup>. Therefore, finding new effective chemotherapeutic agents for OSCC is an urgent task.

Betulinic acid (BA), 3 $\beta$ -hydroxy-lup-20(29)-en-28-oic acid, is a naturally occurring pentacyclic lupane-structured triterpenoid<sup>3</sup> that is found in many fruits, plants, and vegetables, such as birch tree bark (*Betula* sp.), sycamore and the bark of plane trees (*Platanus* sp.), and eucalyptus bark<sup>4,5</sup>. It was found that BA possesses numerous biological properties such as cardioprotective, anti-inflammatory,

immunomodulatory, glucose lowering, anti-HIV, antimalarial, antiangiogenic, antifibrotic, and hepatoprotective<sup>4,6-9</sup>. In particular, recent evidence has supported that BA exhibits an antitumor effect<sup>10</sup>. Liebscher et al. found that BA exhibited inhibitory effects on melanoma cell lines<sup>11</sup>. BA was found to kill colon cancer stem cells via the inhibition of the stearyl-CoA desaturase<sup>12</sup>. Yang et al. discovered that BA inhibited the growth of hepatocellular carcinoma<sup>13</sup>. Moreover, BA and its derivatives possess proapoptotic activities in various cancer cells, including hepatocellular carcinoma<sup>13</sup>, leukemia HL-60 cells<sup>14</sup>, and colon carcinoma cells<sup>15</sup>. It has been shown that BA alone inhibited cell survival and affected cell survival additively in combination with irradiation and decreased clonogenic survival in head and neck squamous cell carcinoma (HNSCC) cells<sup>16</sup>. However, whether BA exhibits an antitumor effect in OSCC is still not known.

<sup>1</sup>These authors provided equal contribution to this work.

Address correspondence to Guang Zeng, Department of Plastic and Burn Surgery, Tangdu Hospital, Fourth Military Medical University, 1 Xinsi Road, Xi'an 710038, P.R. China. E-mail: zengguang10@sina.com

In the current study, we designed the experiments to explore the effects of BA on OSCC cell proliferation *in vitro* and implanted tumor growth *in vivo* and to examine the possible molecular mechanisms. The results showed that BA dose-dependently inhibited cancer cell proliferation *in vitro* and tumor growth in mice.

## MATERIALS AND METHODS

### *Chemicals and Reagents*

p53, signal transducer and activator of transcription 3 (STAT3), p-STAT3, and  $\beta$ -actin antibodies were purchased from Santa Cruz Biotechnology (Santa Cruz, CA, USA). BA, *N*-acetyl-cysteine (NAC), and most of the chemicals and reagents used in this study were procured from Sigma-Aldrich (St. Louis, MO, USA).

### *Cell Culture*

The human OSCC-derived cell line KB was purchased from ATCC (Manassas, VA, USA). Cells were cultured in Dulbecco's modified Eagle's medium (DMEM) containing 10% heat-inactivated fetal bovine serum (FBS), 50 U/ml penicillin, and 50 U/ml streptomycin. Cells were incubated at 37°C in a 5% humidified CO<sub>2</sub>-enriched atmosphere.

### *Cell Transfection and Reporter Gene*

For some experiments, cells were transfected with lentivirus (LV) vector or LV-shp53. Cells in which p53 was stably knocked down were purified by puromycin. For reporter gene experiments, cells were seeded into 12-well plates at a density of  $5 \times 10^4$  cells per well prior to transfection. Cells were transfected with p-p53-TA-luc, p-STAT3-TA-luc, or control vector using Lipofectamine<sup>®</sup> 3000 reagent (Thermo Scientific, Waltham, MA, USA). Twenty-four hours after the transfection, cells were treated with BA for an additional 24 h. Cells were lysed with 1× reporter lysis buffer. Luciferase activity was determined using the Dual-Luciferase<sup>®</sup> Reporter Assay System. The results were expressed as folds of transactivation.

### *Determination of Cell Proliferation*

Cell proliferation was determined using cell counting kit-8 (CCK-8) assay kit (Beyotime, P.R. China) according to the manufacturer's instructions. Cells were plated in 96-well culture plates at a density of  $3 \times 10^4$  and exposed to BA for the indicated time periods. After treatment, 10  $\mu$ l of the CCK-8 solution was added to each well, and cells were cultured at 37°C for an additional hour. Absorbance at 450 nm was measured to evaluate cell proliferation.

### *Determination of Apoptosis*

Apoptosis was determined using TdT-mediated dUTP nick-end labeling (TUNEL) assay kit (Roche) according to the manufacturer's instructions. After the treatment, cells were collected and stained with TUNEL solution.

Cells were then analyzed using flow cytometry. The percentage of apoptotic cells was counted, and the results were shown as folds of control.

### *Determination of Caspase 3 and Caspase 9 Activities*

Pellets of  $1-5 \times 10^6$  cells were suspended in chilled cell lysis buffer. Cytosolic protein from the cells was extracted, and protein concentration was determined. Cell lysis buffer (50  $\mu$ l) containing 50–200  $\mu$ g of protein was used for each assay. Colorimetric assay kits specific for caspase 3 and caspase 9 were used to analyze the activities (BioVision, Milpitas, CA, USA). Absorbance at 405 nm was measured using a microtiter plate reader.

### *Measurement of Oxygen Consumption Rate*

Mitochondria were isolated from the cells using an assay kit (Thermo Scientific) according to the manufacturer's instructions. Mitochondria were resuspended in oxygen-saturated Dulbecco's phosphate-buffered saline (dPBS). Oxygen consumption determination was performed using a Clark electrode (Hansatech Instruments, UK). Oxygen consumption was recorded for 10 min. Results were expressed as a percentage of baseline.

### *Cell Cycle Measurement*

For cell cycle analysis, cells were harvested, fixed in 100% ice-cold ethanol, washed, and incubated in 1 mg/ml propidium iodide (PI) with RNase A (200  $\mu$ g/ml). Cell cycle distribution was analyzed by flow cytometry (C6; BD Biosciences, San Jose, CA, USA).

### *Determination of ROS Generation*

Dihydroethidium (DHE) was used to detect reactive oxygen species (ROS) generation. After treatment, the cells were incubated with 10  $\mu$ M DHE in serum-free culture medium in the dish for 20 min. Fluorescence was then observed under confocal microscopy, and images were captured. In addition, cells were harvested and resuspended in serum-free culture medium at a density of  $1 \times 10^6$  cell. Cells were then incubated with 10  $\mu$ M DHE at 37°C for 30 min. Afterward, cells were washed twice with PBS and analyzed using flow cytometry (C6; BD Biosciences).

### *Quantitative Real-Time PCR*

Total RNA was extracted using TRIzol reagent and retrotranscribed after DNase I (Roche, Switzerland) treatment using a FastQuant RT Kit (TIANGEN, P.R. China). Real-time PCR was performed for 45 cycles with SYBR Green PCR Master Mix (TaKaRa, Japan) and processed on CFX 96 system (Bio-Rad, Hercules, CA, USA) as previously described<sup>17</sup>. Cycle conditions were as follows: initial denaturation at 95°C for 15 min followed by 44 cycles of denaturation at 95°C for 30 s, annealing at 59°C for

30 s, extension at 72°C for 30 s, and plate reading. After the cycles, a dissociation curve was generated from 55°C to 95°C with readings every 0.5°C. Reactions were run in triplicate for each sample. Threshold cycles (Ct) for each tested gene were normalized to the housekeeping  $\beta$ -actin gene value ( $\Delta$ Ct), and every experimental sample was referred to its control ( $\Delta\Delta$ Ct). Fold change values were expressed as  $2^{-\Delta\Delta$ Ct}.

#### Western Blot Analysis

Cells or tumor tissues were lysed using lysis reagent, and proteins were separated using SDS-PAGE gels and then transferred to a PVDF membrane (Millipore, Boston, MA, USA) for immunoblot analysis. Membranes were blocked with 5% fat-free milk in TBS solution for 1 h at room temperature. Membranes were incubated with primary antibodies in TBS containing 5% fat-free milk at 4°C overnight. Unbound primary antibodies were removed by TBS-T washes four times with 15 min each wash. Then membranes were incubated with the horseradish peroxidase (HRP)-conjugated secondary antibodies (Thermo Scientific), which were diluted in TBS-T. Unbound secondary antibodies were removed by TBS-T washes for four times with 15 min for each wash. Proteins were visualized using a chemiluminescent HRP Substrate (Thermo Scientific) according to the manufacturer's protocols. Bands were detected using a Bio-Rad system.

#### Chromatin Immunoprecipitation (ChIP) Assays

A ChIP assay kit (Thermo Scientific) was used to evaluate the binding of p53 to the promoter of Bax according to the manufacturer's protocols. After treatment, chromatin was cross-linked with 1% formaldehyde for 10 min at room temperature. After washing twice, cells were resuspended in the lysis buffer and were sheared to an average DNA fragment length of 100–800 bp by sonication. Normal IgG was used as a negative control, and antibodies against p53 were used for each immunoprecipitation. The precipitated DNA was amplified by real-time PCR for fragments of the Bax promoter.

#### Animal Treatment

Animal treatment was approved by the Animal Care and Use Committee of Tangdu Hospital, Fourth Military Medical University. Sixty male Balb/c nude mice (4–6 weeks old) were injected with KB cells ( $1 \times 10^7$  cells per mouse) in the dorsal flank to create implanted subcutaneous tumors. When the implanted tumors were large enough to measure volume, the mice were randomly allocated into four groups ( $n=15$  in each group): control, 50 mg/kg BA, 75 mg/kg BA, and 150 mg/kg BA. In BA groups, mice were intraperitoneally injected with the indicated dosages of BA (dissolved in normal saline containing 1% DMSO) daily. Mice in the control group

received vehicle. Tumors were examined, and tumor volumes were calculated using the formula  $V=1/2ab^2$  ( $a$ , the largest diameter;  $b$ , the smallest diameter). The experimental period was 3 weeks. At the end of 3 weeks, the animals were sacrificed, and the tumors were collected for mRNA and protein expression.

#### Statistical Analysis

All experiments were performed at least three times, and results were expressed as means  $\pm$  SEM. The results were analyzed by one-way ANOVA followed by a Tukey's test for multiple comparisons. GraphPad Prism software was used to perform statistical analyses. Data were considered statistically significant with a value of  $p < 0.05$ .

## RESULTS

#### BA Inhibits KB Cell Proliferation In Vitro

To test the effect of BA on OSCC cell proliferation, KB cells were incubated with 12.5–100  $\mu$ M BA for 24–72 h. The results showed that BA concentration- and time-dependently inhibited the proliferation of KB cells (Fig. 1). Incubation of cells with 100  $\mu$ M BA for 24 h decreased cell proliferation to nearly 25% of control (Fig. 1). In the experiments for mechanism investigation, 100  $\mu$ M BA was selected to incubate cells for 24 h. The data indicated that BA exhibited an antitumor effect on OSCC cells in vitro.

#### BA Increases Mitochondrial Apoptosis and Induces $G_0/G_1$ Cell Cycle Arrest In Vitro

To explore the mechanism of BA-induced inhibition of OSCC cell proliferation, apoptosis and cell cycle distribution were examined. BA significantly increased TUNEL<sup>+</sup> cells in KB cells, which was concentration dependent (Fig. 2A and B). Activities of caspase 3 and caspase 9 were increased by BA in a concentration-dependent manner (Fig. 2C and D). In addition, Bax (Bcl-2-like protein 4) and B-cell lymphoma 2 (Bcl-2) mRNA expressions were determined by real-time PCR. BA concentration-dependently increased the mRNA expression of Bax and decreased the mRNA expression of Bcl-2 (Fig. 2E and F). Moreover, mitochondrial function was evaluated by determination of oxygen consumption rate. BA dose-dependently decreased the oxygen consumption rate, indicating that BA induced a significant mitochondrial dysfunction (Fig. 2G). Overall, the results demonstrated that BA resulted in notable mitochondrial apoptosis.

Furthermore, cell cycle distribution was determined after BA exposure. BA (50 and 100  $\mu$ M) markedly increased cell number in the  $G_0/G_1$  phase and decreased cell number in the S phase, indicating that BA resulted in a significant  $G_0/G_1$  cell cycle arrest, leading to inhibition of  $G_1/S$  cell cycle transition (Fig. 3A). In the next step,

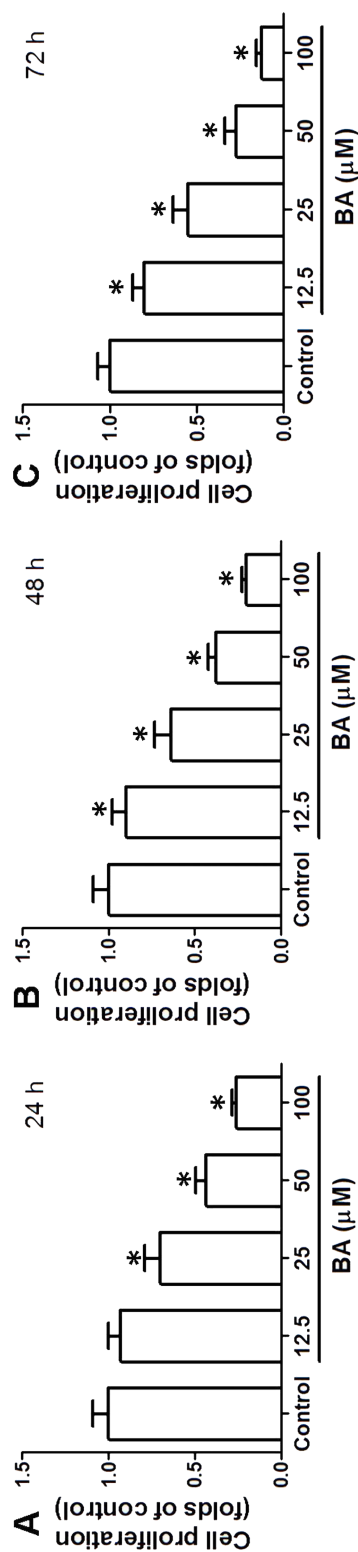


**Figure 1.** Effect of betulinic acid (BA) on cell proliferation in KB cells. KB cells were incubated with 12.5–100  $\mu\text{M}$  BA for 24 h (A), 48 h (B), and 72 h (C). Cell proliferation was detected by a cell counting kit-8 (CCK-8) assay kit. Results were shown as folds of control. \* $p < 0.05$ , compared with that of the control.

we examined the mRNA expression of key regulators responsible for the  $G_1/S$  cell cycle transition, including cyclin D1, cyclin E1, cyclin-dependent kinase 2 (CDK2), CDK4, and CDK6. The results showed that 50 and 100  $\mu\text{M}$  BA significantly decreased the mRNA expression of cyclin D1, but had no significant effect on cyclin E1, CDK2, CDK4, or CDK6 mRNA expression. The results demonstrated that BA induced significant  $G_0/G_1$  cell cycle arrest via regulation of cyclin D1.

#### *ROS Generation Is Involved in BA-Induced Inhibition of Cell Proliferation*

In the next step, we tested whether BA promoted ROS generation in KB cells. BA significantly increased DHE fluorescence in KB cells, indicating that BA increased ROS generation, which was in a concentration-dependent manner (Fig. 4A and B). To test the role of ROS generation in BA-induced inhibition of KB cell proliferation, we used a potent antioxidant, NAC. BA induced an increase in apoptosis and  $G_0/G_1$  cell cycle arrest, and inhibition of cell proliferation was significantly suppressed by NAC (Fig. 4C–E). The results demonstrated that ROS production was involved in the BA-exhibited antitumor effect in KB cells.

#### *p53 Is Involved in BA-Induced Inhibition of Cell Proliferation*

To examine whether p53 was involved in the effect of BA on KB cell proliferation, mRNA and protein expression of p53 in cells treated by BA was determined. BA concentration-dependently increased the mRNA and protein expression of p53 in KB cells (Fig. 5A and B). In the next step, we examined the possible binding of p53 in the promoter of Bax. BA significantly increased the content of Bax after p53 baiting, which was concentration dependent (Fig. 5C). Moreover, reporter gene activity was conducted to evaluate Bax transcription regulated by p53. We showed that BA treatment significantly increased reporter gene activity of p53 in KB cells (Fig. 5D). To further prove the pivotal role of p53 in mediating the inhibitory effect of BA on cell proliferation, KB cells were transfected with LV-shp53. LV-shp53 transfection notably and stably decreased the expression of p53 in KB cells (Fig. 5E). Knockdown of p53 remarkably inhibited the effect of BA on apoptosis, cell cycle arrest, and cell proliferation (Fig. 5F–H). The data demonstrated that p53 mediated BA-induced apoptosis, cell cycle arrest, and final inhibition of cell proliferation. Furthermore, we examined the possible relationship between ROS generation and upregulation of p53 in response to BA. Antioxidant NAC significantly suppressed the BA-induced increase in p53 mRNA and protein expression, indicating that ROS was responsible for the upregulation of p53 induced by BA (Fig. 5I and J).

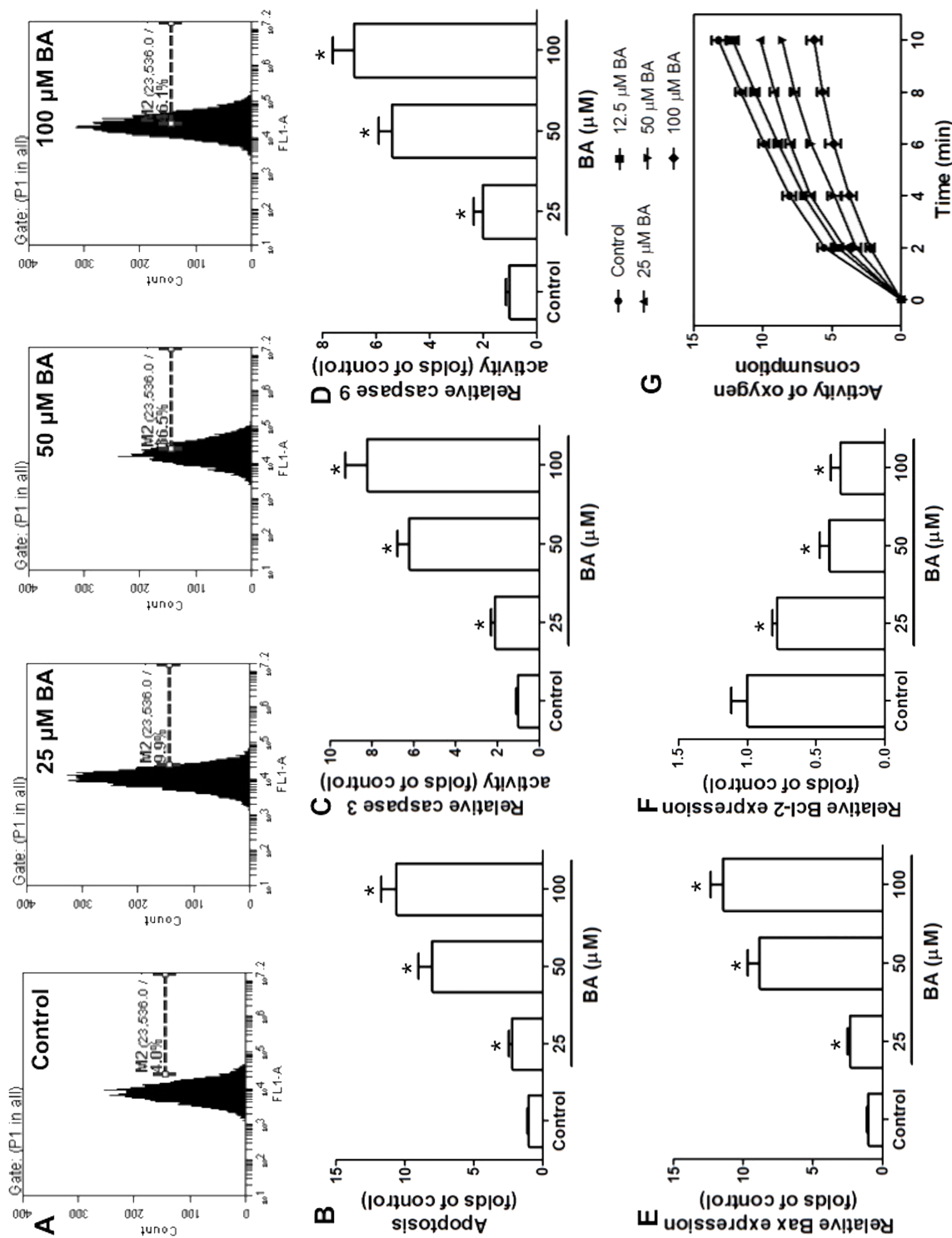


**Figure 2.** Effect of BA on mitochondrial apoptosis in KB cells. KB cells were incubated with indicated concentrations of BA for 24 h. (A, B) Apoptosis was analyzed by flow cytometry using a TdT-mediated dUTP nick-end labeling (TUNEL) assay kit, and results are shown as folds of control. (C, D) Activities of caspase 3 and caspase 9 were measured using commercial kits. (E, F) mRNA expression of Bax and Bcl-2 was examined by real-time PCR. (G) Mitochondria were isolated, and oxygen consumption rate was determined. Activity of oxygen consumption was recorded for 10 min. \* $p < 0.05$ , compared with that of the control.

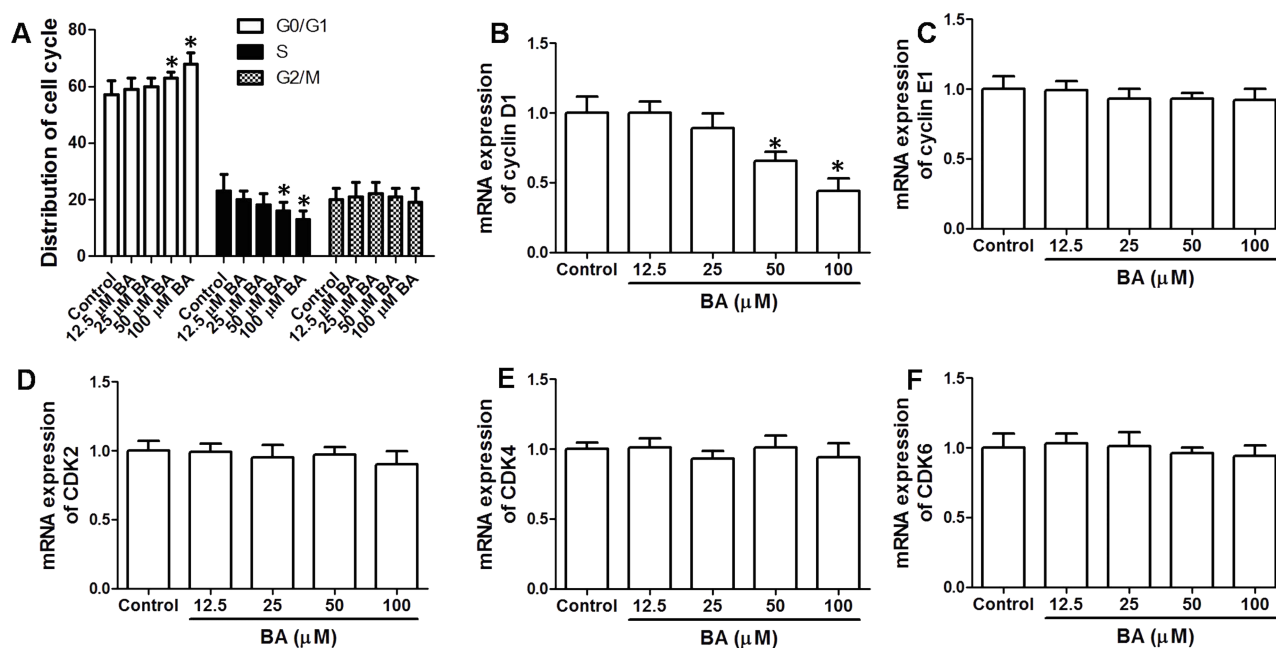


**Figure 3.** Effect of BA on cell cycle distribution in KB cells. KB cells were incubated with the indicated concentrations of BA for 24 h. (A) Cell cycle distribution was determined by propidium iodide (PI) staining and analyzed by flow cytometry. (B–F) mRNA expression of cyclin D1, cyclin E1, CDK2, CDK4, and CDK6 was examined by real-time PCR. Results are shown as folds of control. \* $p < 0.05$ , compared with that of the control.

#### *Inhibition of STAT3 Signaling Is Involved in BA-Induced Suppression of Cell Proliferation*

To examine whether STAT3 signaling was possibly involved in the effect of BA on KB cell proliferation, phosphorylation of STAT3 was examined. BA concentration-dependently decreased the expression of phosphorylated STAT3 in KB cells, indicating the inhibition of STAT3 signaling (Fig. 6A). Moreover, STAT3 luciferase activity was decreased by BA in a concentration-dependent manner, confirming the inhibition of STAT3 transcriptional activity (Fig. 6B). Based on the reported role of STAT3 signaling in promoting tumor development, the results indicated that blockage of STAT3 signaling may be a possible mechanism of the antitumor effect of BA. Furthermore, BA-induced inhibition of phosphorylation of STAT3 was suppressed by NAC (Fig. 6C), implying that ROS generation was involved in the inhibition of STAT3 signaling induced by BA.

#### *Antitumor Effect of BA In Vivo*

Furthermore, we tested the antitumor effect of BA against OSCC in implanted mice *in vivo*. The results showed that a 3-week administration of BA dose-dependently inhibited the increase in tumor volume in nude mice (Fig. 7A). It was demonstrated that BA exhibited an antitumor effect against OSCC both *in vitro* and *in vivo*. In addition, mRNA expression of p53 in implanted tumor

tissues was decreased by BA in a dose-dependent manner (Fig. 7B). Phosphorylation of STAT3 in tumor tissues declined as the dose of BA increased, compared with that of the control (Fig. 7C). The results demonstrated that upregulation of p53 and inhibition of STAT3 signaling may be involved in the antitumor effect of BA against OSCC in implanted tumor development.

## DISCUSSION

Cancer development is closely associated with the enhancement of cancer cells and the dysregulation of apoptotic cell death<sup>18</sup>. Defects in apoptotic signaling are usually considered to be a hallmark of malignant tumors, which contributes to abnormal cell survival<sup>19,20</sup>. Therefore, induction of apoptosis is often used as a strategy for the investigation of antitumor drugs<sup>21</sup>. Apoptosis, also called programmed cell death, could occur through the cell death receptor-mediated extrinsic signaling and mitochondrial caspase-mediated intrinsic pathways<sup>22,23</sup>. In response to stress stimuli, mitochondria may release proteins such as cytochrome c to cytosol, where these proteins activate caspase cascades, leading to apoptotic cell death<sup>24</sup>. Mitochondrial apoptosis is highly regulated by Bcl-2 protein family members<sup>21</sup>, which can be subdivided into proapoptotic effector proteins (such as Bax), proapoptotic BH3-only proteins, and antiapoptotic Bcl-2 proteins (such

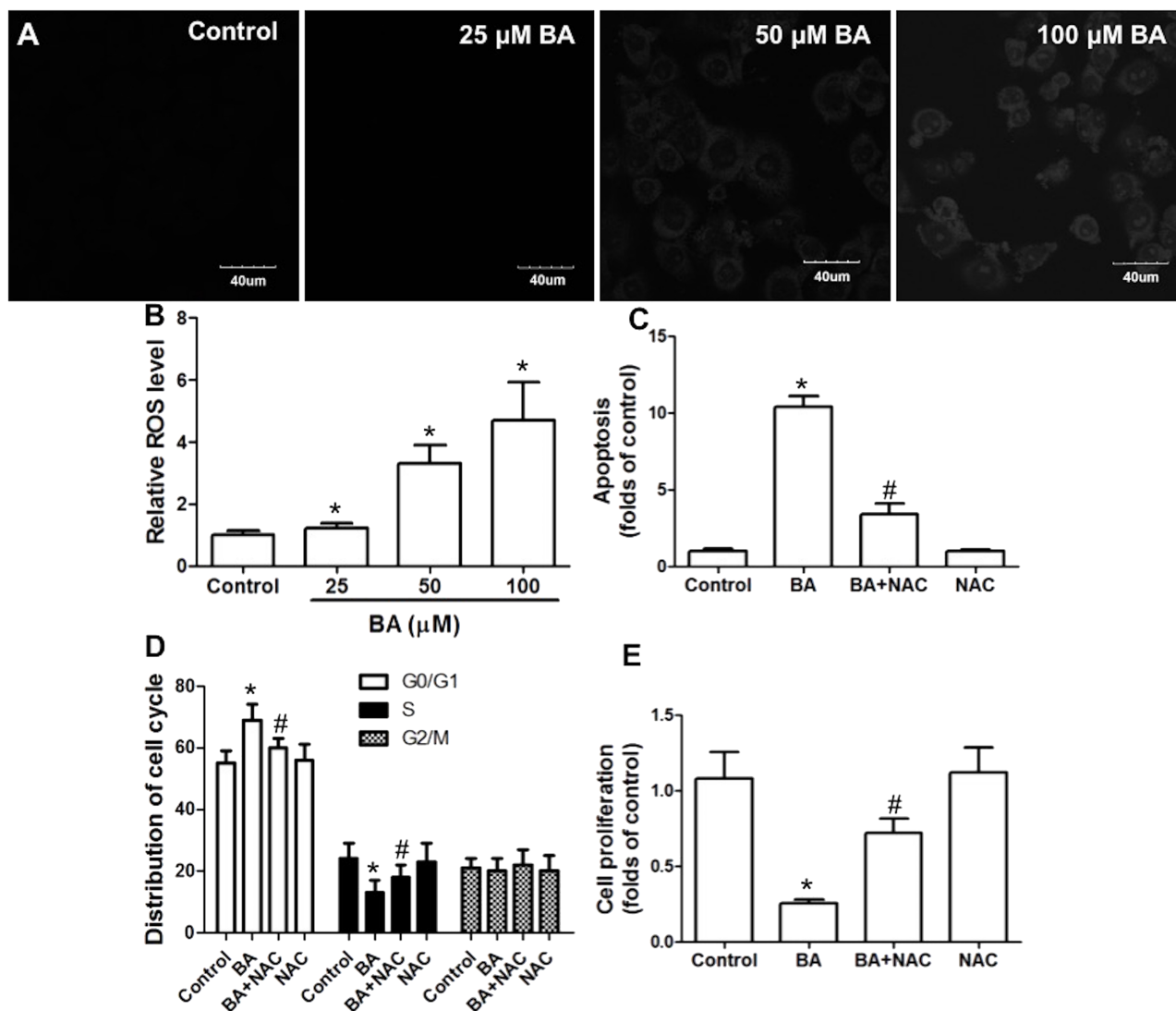


**Figure 4.** Role of reactive oxygen species (ROS) generation in the antitumor effect of BA in vitro. KB cells were incubated with the indicated concentrations of BA for 24 h. (A, B) Cells were stained with dihydroethidium (DHE), and ROS level was observed by microscopy (A) or analyzed by flow cytometry (B). KB cells were exposed to 100  $\mu\text{M}$  BA in the presence or absence of 100  $\mu\text{M}$  *N*-acetyl-cysteine (NAC) for 24 h. Apoptosis was examined by TUNEL assay (C), cell cycle distribution was measured by PI staining (D), and cell proliferation was determined by the CCK-8 kit (E). \* $p < 0.05$ , compared with that of the control. # $p < 0.05$ , compared with that of the BA group.

as Bcl-2). Mitochondrial function is critical for the maintenance of the balance of apoptosis. Once mitochondrial dysfunction is induced, the mitochondrial molecular events may be initiated, resulting in final apoptotic cell death<sup>25,26</sup>.

It is shown that BA could exhibit an inhibitory effect on cell proliferation in several cancer cell lines. Proapoptotic effects of BA have been found by some research groups. Eichenmuller et al. found that BA treatment promoted apoptosis in hepatoblastoma cells<sup>27</sup>. A novel triazole derivative of BA was shown to induce extrinsic and intrinsic apoptosis in human leukemia HL-60 cells<sup>14</sup>. In the present

study, we investigated the effect of BA on OSCC cell proliferation in KB cells and implanted tumor growth in nude mice. The results showed that BA could dose-dependently inhibit tumor cell proliferation in vitro and suppress tumor growth in vivo, indicating that BA exhibited an antitumor effect against OSCC. Moreover, the effect of BA on mitochondrial apoptosis was assessed. We showed that BA exhibited proapoptotic activities in OSCC cells, as reflected by an increase in TUNEL-staining cells and caspase 3 and caspase 9 activities, increase in Bax mRNA expression, decrease in Bcl-2 mRNA expression,

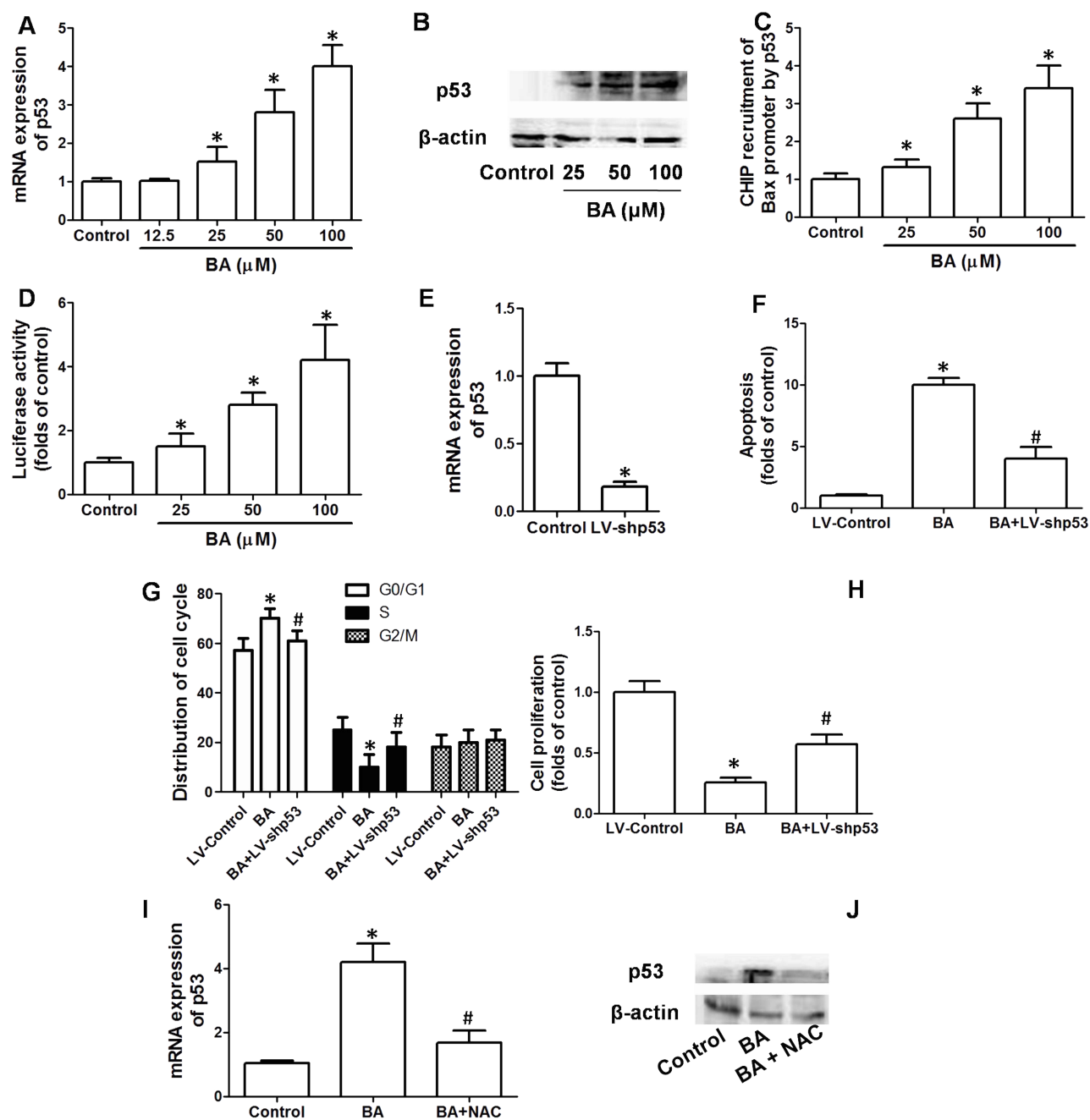


**Figure 5.** Role of p53 in the antitumor effect of BA in vitro. KB cells were incubated with the indicated concentrations of BA for 24 h. (A, B) mRNA and protein expression of p53 were determined by real-time PCR and Western blot, respectively. (C) p53 binding in the promoter of Bax was examined by chromatin immunoprecipitation (ChIP) assay, and results are shown as folds of Bax promoter expression in the control group. (D) Reporter gene activity of p53 was examined and shown as relative activity of the control group. KB cells were transfected with LV-shp53 to knock down p53 expression. Cells in which p53 was stably knocked down were exposed to 100  $\mu\text{M}$  BA for 24 h. (E) mRNA expression of p53 was measured to evaluate the efficiency of p53 knockdown. Apoptosis was examined by TUNEL assay (F), cell cycle distribution was measured by PI staining (G), and cell proliferation was determined by the CCK-8 kit (H). KB cells were exposed to 100  $\mu\text{M}$  BA in the presence or absence of 100  $\mu\text{M}$  NAC for 24 h. mRNA and protein expression of p53 were determined by real-time PCR and Western blot (I, J), respectively. \* $p < 0.05$ , compared with that of the control. # $p < 0.05$ , compared with that of the BA group.



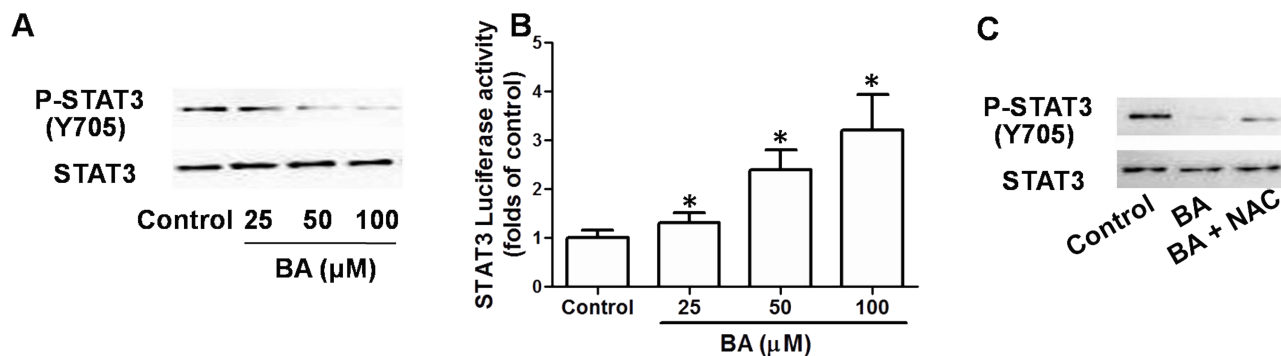


**Figure 6.** Role of inhibition of signal transducer and activator of transcription 3 (STAT3) signaling in the antitumor effect of BA in vitro. KB cells were incubated with indicated concentrations of BA for 24 h. (A) Phosphorylation of STAT3 was determined by Western blot. (B) Reporter gene activity of STAT3 was examined and shown as a relative activity of the control group. KB cells were exposed to 100 μM BA in the presence or absence of 100 μM NAC for 24 h. Phosphorylation of STAT3 was determined by Western blot (C). \**p*<0.05, compared with that of the control.

and decrease in oxygen consumption rate. The results demonstrated that activation of mitochondrial apoptotic cell death may be involved in the antitumor effect of BA.

Cell cycle transition is pivotal for cell proliferation in both normal cells and cancer cells<sup>28</sup>. Inhibition of cell

cycle progression is also considered for the development of anticancer drugs<sup>28</sup>. In this study, we examined the effect of BA on cell cycle distribution. We showed that a high level of BA induced G<sub>0</sub>/G<sub>1</sub> cell cycle arrest, as evidenced by a significant increase in G<sub>0</sub>/G<sub>1</sub> phase cell

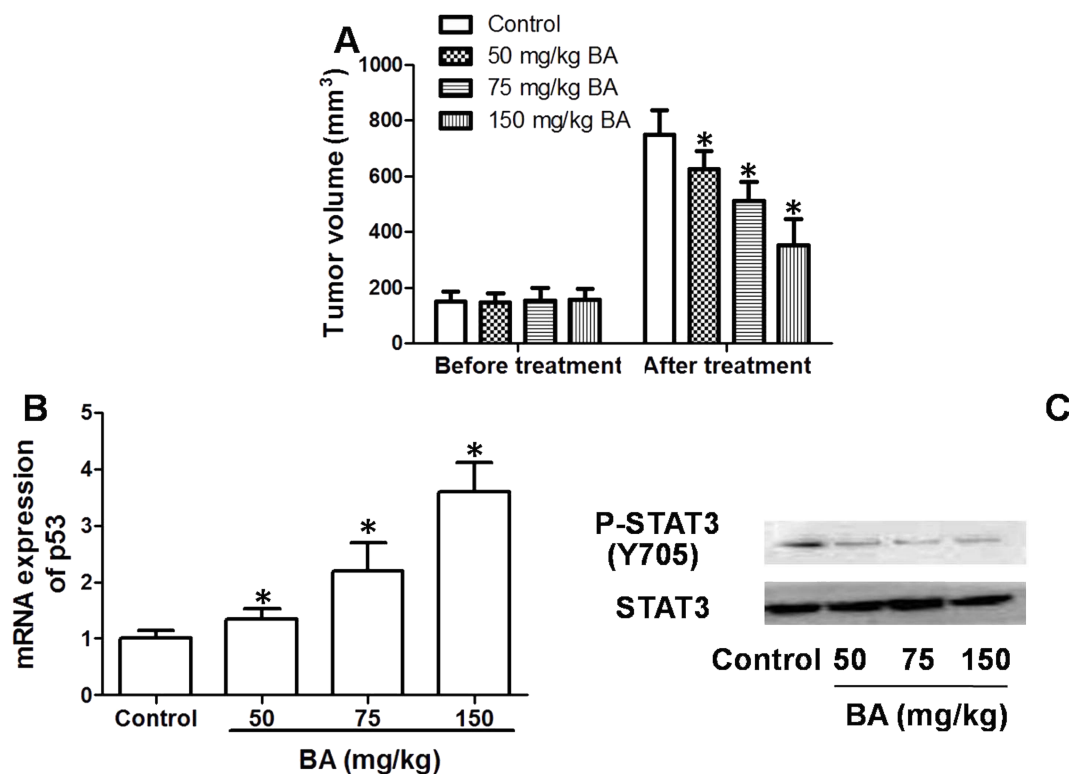


**Figure 7.** Antitumor effect of BA in vivo. Mice (15 in each group) were implanted with tumors and treated with 50–150 mg/kg BA for 3 weeks. (A) Tumor volumes were calculated. (B) mRNA of p53 in tumors were determined by real-time PCR. (C) Phosphorylation of STAT3 in tumors was determined by Western blot. \**p*<0.05, compared with that of the control.

numbers and a decrease in S phase cell population. G<sub>1</sub>/S cell cycle transition is controlled by several key regulators, including cyclin D and cyclin E, CDK2, CDK4, and CDK6<sup>29</sup>. In our study, we detected the expression of these key proteins. We found that BA mainly increased the mRNA expression of cyclin D1 but had no significant effect on cyclin E, CDK2, CDK4, or CDK6 expression. These results demonstrated that a deficiency in cyclin D1-mediated G<sub>0</sub>/G<sub>1</sub> cell cycle arrest may be involved in the antitumor effect of BA in OSCC.

ROS is a group of highly reactive substances that could damage a variety of molecules or alter a battery of signaling pathways<sup>30,31</sup>. Increased production of ROS has been believed to be an important determinant of the occurrence of apoptosis. Promotion of ROS generation plays a crucial role in chemopreventive effects against numerous antitumor agents<sup>32–34</sup>. In addition, BA was found to generate ROS in several cell lines<sup>13,35,36</sup>. In the current study, we tested the possible role of ROS in the antitumor effect of BA in OSCC. We showed that BA concentration-dependently increased ROS generation. Amelioration of ROS by antioxidant NAC treatment markedly suppressed the inhibitory effect of BA on cell proliferation, the induction of apoptosis, and G<sub>0</sub>/G<sub>1</sub> cell cycle arrest. The results demonstrated that ROS generation contributes to the antitumor effect of BA in OSCC.

p53, a well-known tumor suppressor gene, is regarded as the “guardian of the genome” and plays a crucial role in controlling cell cycle checkpoints and apoptosis via regulation of a battery of target genes<sup>37</sup>. Previous studies have shown that activation of p53 was involved in BA-induced apoptosis in hepatocellular carcinoma<sup>13</sup>. In our study, we examined the possible role of p53 in the regulation of apoptosis, cell cycle arrest, and cell proliferation. We found that BA dose-dependently increased p53 expression in KB cells, and knockdown of p53 significantly inhibited BA-induced apoptosis, cell cycle arrest, and inhibition of cell proliferation. Moreover, BA increased the reporter gene activity of p53 and the binding activity of p53 in Bax promoters. Furthermore, antioxidant NAC treatment suppressed the BA-induced increase in p53. These results demonstrated that ROS-mediated upregulation of p53 and subsequent activation of mitochondrial apoptosis and G<sub>0</sub>/G<sub>1</sub> cell cycle arrest were responsible for BA-induced inhibition of cell proliferation.

STAT3 is an important transcription factor that is over-expressed in several types of cancer, and inhibition of STAT3 signaling has been shown to inhibit oral cancer development<sup>38–41</sup>. Persistent activation of STAT3 could increase cancer cell proliferation and tumor growth through the regulation of antiapoptotic and cell cycle-regulating proteins<sup>42,43</sup>. In this study, we tested the effect of BA on STAT3 signaling. We found that BA could evidently

inhibit STAT3 signaling, as evidenced by the decrease in STAT3 phosphorylation in OSCC cells and in implanted tumors in nude mice. Moreover, BA-induced decrease in STAT3 phosphorylation was suppressed by NAC, indicating that ROS generation was involved in BA-induced regulation of STAT3 signaling, which is a possible mechanism of BA-exhibited antitumor effect.

In conclusion, in the current study we examined the effect of BA on cell proliferation in OSCC cells and on tumor growth in implanted tumor in nude mice. The results showed that BA exhibited dose-dependent antitumor activity both in vitro and in vivo. BA promoted ROS production, increased p53 expression and the transcription of proapoptotic regulator, and inhibited STAT3 signaling, resulting in promotion of mitochondrial apoptosis, induction of cell cycle arrest, and final inhibition of cell proliferation. Taken together, the data demonstrated that ROS-p53 signaling was crucial for the BA-exhibited antitumor effect in OSCC. Further studies are warranted to make a comprehensive evaluation on the clinical value of BA as a novel anti-OSCC agent.

*ACKNOWLEDGMENT:* This work was supported by The National Natural Science Foundation of China (No. 81502337). The authors declare no conflicts of interest.

## REFERENCES

1. Warnakulasuriya S. Global epidemiology of oral and oropharyngeal cancer. *Oral Oncol.* 2009;45:309–16.
2. Petersen PE. Oral cancer prevention and control—The approach of the World Health Organization. *Oral Oncol.* 2009;45:454–60.
3. Moghaddam MG, Ghaffari AFBH. Various botanical sources of betulinic acid: A review. *Asian J Chem.* 2012; (24):4843–6.
4. Csuk R. Betulinic acid and its derivatives: A patent review (2008-2013). *Expert Opin Ther Pat.* 2014;24:913–23.
5. Bhatti HN, Khera RA. Biotransformations of diterpenoids and triterpenoids: A review. *J Asian Nat Prod Res.* 2014;16: 70–104.
6. Laszczyk MN. Pentacyclic triterpenes of the lupane, oleanane and ursane group as tools in cancer therapy. *Planta Med.* 2009;75:1549–60.
7. Xia A, Xue Z, Li Y, Wang W, Xia J, Wei T, Cao J, Zhou W. Cardioprotective effect of betulinic acid on myocardial ischemia reperfusion injury in rats. *Evid Based Complement Alternat Med.* 2014;2014:573745.
8. Nader MA, Baraka HN. Effect of betulinic acid on neutrophil recruitment and inflammatory mediator expression in lipopolysaccharide-induced lung inflammation in rats. *Eur J Pharm Sci.* 2012;46:106–13.
9. Liu CM, Qi XL, Yang YF, Zhang XD. Betulinic acid inhibits cell proliferation and fibronectin accumulation in rat glomerular mesangial cells cultured under high glucose condition. *Biomed Pharmacother.* 2016;80:338–42.
10. Yogeewari P, Sriram D. Betulinic acid and its derivatives: A review on their biological properties. *Curr Med Chem.* 2005;12:657–66.

11. Liebscher G, Vanchangiri K, Mueller T, Feige K, Cavalleri JM, Paschke R. In vitro anticancer activity of betulinic acid and derivatives thereof on equine melanoma cell lines from grey horses and in vivo safety assessment of the compound NVX-207 in two horses. *Chem Biol Interact.* 2016;246:20–9.
12. Potze L, di Franco S, Kessler JH, Stassi G, Medema JP. Betulinic acid kills colon cancer stem cells. *Curr Stem Cell Res Ther.* 2016;11:427–33.
13. Yang J, Qiu B, Li X, Zhang H, Liu W. p53-p66(shc)/miR-21-Sod2 signaling is critical for the inhibitory effect of betulinic acid on hepatocellular carcinoma. *Toxicol Lett.* 2015;238:1–10.
14. Khan I, Guru SK, Rath SK, Chinthakindi PK, Singh B, Koul S, Bhushan S, Sangwan PL. A novel triazole derivative of betulinic acid induces extrinsic and intrinsic apoptosis in human leukemia HL-60 cells. *Eur J Med Chem.* 2016;108:104–16.
15. Chakraborty B, Dutta D, Mukherjee S, Das S, Maiti NC, Das P, Chowdhury C. Synthesis and biological evaluation of a novel betulinic acid derivative as an inducer of apoptosis in human colon carcinoma cells (HT-29). *Eur J Med Chem.* 2015;102:93–105.
16. Eder-Czembirek C, Erovcic BM, Czembirek C, Brunner M, Selzer E, Potter R, Thurnher D. Betulinic acid a radiosensitizer in head and neck squamous cell carcinoma cell lines. *Strahlenther Onkol.* 2010;186:143–8.
17. Onesto E, Colombrita C, Gumina V, Borghi MO, Dusi S, Doretti A, Fagiolari G, Invernizzi F, Moggio M, Tiranti V, Silani V, Ratti A. Gene-specific mitochondria dysfunctions in human TARDBP and C9ORF72 fibroblasts. *Acta Neuropathol Commun.* 2016;4:47.
18. Albers AE, Strauss L, Liao T, Hoffmann TK, Kaufmann AM. T cell-tumor interaction directs the development of immunotherapies in head and neck cancer. *Clin Dev Immunol.* 2010;2010:236378.
19. Goldar S, Khaniani MS, Derakhshan SM, Baradaran B. Molecular mechanisms of apoptosis and roles in cancer development and treatment. *Asian Pac J Cancer Prev.* 2015;16:2129–44.
20. Kundu J, Chun KS, Aruoma OI, Kundu JK. Mechanistic perspectives on cancer chemoprevention/chemotherapeutic effects of thymoquinone. *Mutat Res.* 2014;768:22–34.
21. Lopez J, Tait SW. Mitochondrial apoptosis: Killing cancer using the enemy within. *Br J Cancer.* 2015;112:957–62.
22. Tiwari M, Prasad S, Tripathi A, Pandey AN, Ali I, Singh AK, Shrivastav TG, Chaube SK. Apoptosis in mammalian oocytes: A review. *Apoptosis.* 2015;20:1019–25.
23. Wang K. Autophagy and apoptosis in liver injury. *Cell Cycle.* 2015;14:1631–42.
24. Taylor RC, Cullen SP, Martin SJ. Apoptosis: Controlled demolition at the cellular level. *Nat Rev Mol Cell Biol.* 2008;9:231–41.
25. Dou G, Sreekumar PG, Spee C, He S, Ryan SJ, Kannan R, Hinton DR. Deficiency of alphaB crystallin augments ER stress-induced apoptosis by enhancing mitochondrial dysfunction. *Free Radic Biol Med.* 2012;53:1111–22.
26. Liu Z, Song G, Zou C, Liu G, Wu W, Yuan T, Liu X. Acrylamide induces mitochondrial dysfunction and apoptosis in BV-2 microglial cells. *Free Radic Biol Med.* 2015;84:42–53.
27. Eichenmuller M, von Schweinitz D, Kappler R. Betulinic acid treatment promotes apoptosis in hepatoblastoma cells. *Int J Oncol.* 2009;35:873–9.
28. O’Leary B, Finn RS, Turner NC. Treating cancer with selective CDK4/6 inhibitors. *Nat Rev Clin Oncol.* 2016;13:417–30.
29. Neganova I, Lako M. G1 to S phase cell cycle transition in somatic and embryonic stem cells. *J Anat.* 2008;213:30–44.
30. Noctor G, Foyer CH. Intracellular redox compartmentation and ROS-related communication in regulation and signaling. *Plant Physiol.* 2016;171:1581–92.
31. Diebold L, Chandel NS. Mitochondrial ROS regulation of proliferating cells. *Free Radic Biol Med.* 2016;100:86–93.
32. Lim W, Yang C, Bazer FW, Song G. Chrysophanol induces apoptosis of choriocarcinoma through regulation of ROS and the AKT and ERK1/2 pathways. *J Cell Physiol.* 2017;232:331–9.
33. Junior PL, Camara DA, Costa AS, Ruiz JL, Levy D, Azevedo RA, Pasqualoto KF, de Oliveira CF, de Melo TC, Pessoa ND, Fonseca PM, Pereira A, Araldi RP, Ferreira AK. Apoptotic effect of eugenol involves G2/M phase abrogation accompanied by mitochondrial damage and clastogenic effect on cancer cell in vitro. *Phytomedicine.* 2016;23:725–35.
34. Huang Q, Zhan L, Cao H, Li J, Lyu Y, Guo X, Zhang J, Ji L, Ren T, An J, Liu B, Nie Y, Xing J. Increased mitochondrial fission promotes autophagy and hepatocellular carcinoma cell survival through the ROS-modulated coordinated regulation of the NFkB and TP53 pathways. *Autophagy.* 2016;1–16.
35. Dash SK, Chattopadhyay S, Dash SS, Tripathy S, Das B, Mahapatra SK, Bag BG, Karmakar P, Roy S. Self assembled nano fibers of betulinic acid: A selective inducer for ROS/TNF-alpha pathway mediated leukemic cell death. *Bioorg Chem.* 2015;63:85–100.
36. Chakraborty B, Dutta D, Mukherjee S, Das S, Maiti NC, Das P, Chowdhury C. Synthesis and biological evaluation of a novel betulinic acid derivative as an inducer of apoptosis in human colon carcinoma cells (HT-29). *Eur J Med Chem.* 2015;102:93–105.
37. Pflaum J, Schlosser S, Muller M. p53 family and cellular stress responses in cancer. *Front Oncol.* 2014;4:285.
38. Huang JS, Yao CJ, Chuang SE, Yeh CT, Lee LM, Chen RM, Chao WJ, Whang-Peng J, Lai GM. Honokiol inhibits sphere formation and xenograft growth of oral cancer side population cells accompanied with JAK/STAT signaling pathway suppression and apoptosis induction. *BMC Cancer.* 2016;16:245.
39. Baek SH, Ko JH, Lee H, Jung J, Kong M, Lee JW, Lee J, Chinnathambi A, Zayed ME, Alharbi SA, Lee SG, Shim BS, Sethi G, Kim SH, Yang WM, Um JY, Ahn KS. Resveratrol inhibits STAT3 signaling pathway through the induction of SOCS-1: Role in apoptosis induction and radiosensitization in head and neck tumor cells. *Phytomedicine.* 2016;23:566–77.
40. Escobar Z, Bjartell A, Canesin G, Evans-Axelsson S, Sterner O, Hellsten R, Johansson MH. Preclinical characterization of 3beta-(N-acetyl l-cysteine methyl ester)-2-alpha,3-dihydrogaliellalactone (GPA512), a prodrug of a direct STAT3 inhibitor for the treatment of prostate cancer. *J Med Chem.* 2016;59:4551–62.
41. Geiger JL, Grandis JR, Bauman JE. The STAT3 pathway as a therapeutic target in head and neck cancer: Barriers and innovations. *Oral Oncol.* 2016;56:84–92.
42. Masuda M, Suzui M, Yasumatu R, Nakashima T, Kuratomi Y, Azuma K, Tomita K, Komiyama S, Weinstein IB.

- Constitutive activation of signal transducers and activators of transcription 3 correlates with cyclin D1 overexpression and may provide a novel prognostic marker in head and neck squamous cell carcinoma. *Cancer Res.* 2002;62:3351-5.
43. Lin Q, Lai R, Chirieac LR, Li C, Thomazy VA, Grammatikakis I, Rassidakis GZ, Zhang W, Fujio Y, Kunisada K, Hamilton SR, Amin HM. Constitutive activation of JAK3/STAT3 in colon carcinoma tumors and cell lines: Inhibition of JAK3/STAT3 signaling induces apoptosis and cell cycle arrest of colon carcinoma cells. *Am J Pathol.* 2005;167:969-80.